RSC Advances

PAPER

View Article Online
View Journal | View Issue

Check for updates

Cite this: RSC Adv., 2019, 9, 2626

The mechanistic investigations of photochemical decarbonylations and oxidative addition reactions for $M(CO)_5$ (M = Fe, Ru, Os) complexes†

Zheng-Feng Zhang[a] and Ming-Der Su *[ab]

The mechanisms for the photochemical CO-dissociation and the oxidative addition reactions are studied theoretically using three model systems: $M(CO)_5$ (M = Fe, Ru, and Os) and the CASSCF/Def2-SVP (fourteen-electron/ten-orbital active space) and MP2-CAS/Def2-SVP//CASSCF/Def2-SVP methods. The structures of the intersystem crossings and the conical intersections, which play a decisive role in these CO photo-extrusion reactions, are determined. The intermediates and the transition structures in either the singlet or triplet states are also computed, in order to explain the reaction routes. These model studies suggest that after the irradiation of $Fe(CO)_5$ with UV light, it quickly loses one CO molecule to generate a 16-electron iron tetracarbonyl, in either the singlet or the triplet states. It is found that the triplet $Fe(CO)_4$ plays a vital role in the formation of the final oxidative addition product, $Fe(CO)_4(H)(SiMe_3)$, but the singlet $Fe(CO)_4$ plays a relatively minor role in the formation of the final product. However, its vacant coordination site interacts weakly with solvent molecules ($(Me_3)SiH$) to yield the alkyl-solvated iron complexes, which are detectable experimentally. The theoretical observations show that $Ru(CO)_5$ and $Os(CO)_5$ have similar photochemical and thermal potential energy profiles. In particular, this study demonstrates that the oxidative addition yield for Fe is much greater than those for its Ru and Os counterparts, under the same chemical conditions.

Received 14th September 2018
Accepted 7th December 2018

DOI: 10.1039/c8ra07669c

rsc.li/rsc-advances

I. Introduction

Over the past forty years, the photochemistry of coordinatively saturated pentacarbonyl transition-metal complexes that feature the group 8 elements, $M(CO)_5$ (M = Fe, Ru, and Os), has been extensively studied.[1,2] The prevailing photochemical operation for these metal pentacarbonyl compounds is CO ligand dissociation, which produces highly reactive coordination positions at the transition metal center. Therefore, understanding the formation mechanisms and reactivity patterns for these important intermediates is necessary for both the synthetic and catalytic fields of inorganic and organometallic chemistry.

In particular, the photochemistry of $Fe(CO)_5$ has been the subject of study for many years because of its applications in various areas, including photocatalysis and synthesis.[3–10] The photolytic dissociation of a CO ligand from $Fe(CO)_5$ to generate $Fe(CO)_4$ (ref. 11–14) is the most important aspect of its reaction to UV irradiation.[15–25] Starting from this unsaturated 16-electron iron carbonyl intermediate $Fe(CO)_4$, it can easily react with different types of molecules to undergo oxidative addition reactions,[26–28] which are of both academic and commercial importance in inorganic and organometallic chemistry.[29–32] As a consequence, the study of the photochemistry of $Fe(CO)_5$ has been the subject of a great many experimental and theoretical studies that seek to determine the fundamental aspects of its reaction chemistry.[33–37] Along the entire group 8 metal triad (Fe, Ru, and Os), the photochemistry of $Ru(CO)_5$ and $Os(CO)_5$ has not been the subject of extensive study.[38–47] The reason for this could be that iron is cheap and environmentally benign but ruthenium and osmium are expensive and toxic. The instability of the $Ru(CO)_5$ and $Os(CO)_5$ complexes with respect to the respective formation of the well-known $Ru_3(CO)_{12}$ and $Os_3(CO)_{12}$ species could be another reason.[45] Nevertheless, $Fe(CO)_5$ is quite toxic as well.

The available experimental observations show that upon CO-photolysis of the pentacarbonyl metal complex $M(CO)_5$,[2] it yields the coordinatively unsaturated intermediate, $Fe(CO)_4$, which has the triplet ground state. This result has been verified both experimentally[11–25,48–53] and theoretically.[54–61] However, both $Ru(CO)_4$ and $Os(CO)_4$ are predicted to have a singlet ground state.[38–47] In particular, iron tetracarbonyl fragments are an exceedingly active catalyst, as mentioned previously,[11–14,26–28] but ruthenium and osmium tetracarbonyl fragments are not easily formed photochemically from the corresponding $M(CO)_5$

---

[a] Department of Applied Chemistry, National Chiayi University, Chiayi 60004, Taiwan. E-mail: midesu@mail.ncyu.edu.tw

[b] Department of Medicinal and Applied Chemistry, Kaohsiung Medical University, Kaohsiung 80708, Taiwan

† Electronic supplementary information (ESI) available. See DOI: 10.1039/c8ra07669c

reactants, because unlike $Fe(CO)_4$, these can be produced but immediately combine with one CO molecule.[11–14,38–47]

The activation of the Si–H bond in alkylsilane by this a d^8 organometallic photoproduct $Fe(CO)_4$ has been studied using picosecond time-resolved infrared (TRIR) spectroscopy.[62–66] Therefore, if the reactants and products have different spin states, the way in which the species in a particular spin state transform into the final products of the same spin state by way of several intermediates of different spin state and the spin crossovers is of interest.

After several decades of intensive research into the oxidative addition of alkanes on $Fe(CO)_4$,[67–76] much is still not known about its initial CO-photoextrusion mechanism, nor about that for the analogous $Ru(CO)_5$ and $Os(CO)_5$ molecules.[54–63,77–79] It is astonishing how little is understood about the role that is played by the either the photo-generated singlet or triplet unsaturated d^8 $M(CO)_4$ intermediates in the oxidative addition reaction with organic molecules, considering the importance of these tetracarbonyl metal complexes in the fields of catalytic and synthetic chemistry.

In principle, understanding the characteristics of the potential energy surfaces is of great importance in determining the functions of different possible courses. In spite of the large number of photochemical results for the $Fe(CO)_4$ species, which may help in interpreting the potential energy surfaces for pentacarbonyl transition-metal complexes, the entire mechanistic detail remains unexplained. Indeed, it is not possible to locate intermediates or the transition states because of the limitations of current experimental techniques. Theoretical computations, which are a major source of dependable essential information, are an extremely useful tool with which to study the photochemistry so a theoretical study of the mechanisms for the photodissociation of d^8 $M(CO)_5$ (M = Fe, Ru, and Os) and the Si–H bond–activation reaction for correspondingly photogenerated $M(CO)_4$ with trimethylsilane, eqn (1), is undertaken.

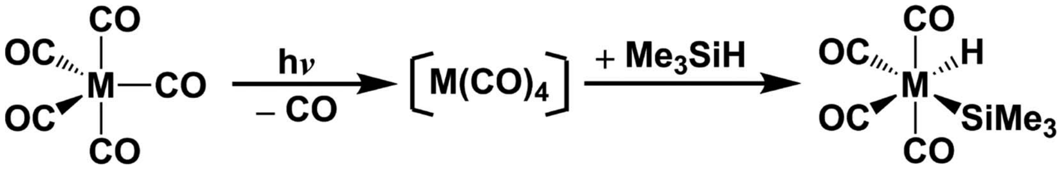

(1)

This theoretical study demonstrates that either the spin crossover (usually from the triplet excited state to the singlet ground state) or the conical intersection (generally from the singlet excited state to the singlet ground state)[80–85] mechanisms play a vital role in interpreting the mechanisms for the photochemical oxidative addition reactions for the pentacarbonyl transition-metal complexes, $M(CO)_5$ (M = Fe, Ru, and Os). The theoretical results for all three transition metals are also compared to determine the implications for the photochemistry of iron, ruthenium and osmium pentacarbonyl molecules. This study gives a better understanding of the photochemical reactions of the group 8 triad, $M(CO)_5$, and supports experimental observations.[2,11–14,38–47]

II. Methodology

The intersection points for the ground state (S_0), the first singlet excited state (S_1) and the lowest triplet excited state (T_1) surfaces and the transition states and the local minima for the photochemical reactions of d^8 $M(CO)_5$ complexes (eqn (1)) on S_0, S_1 and T_1 surfaces are determined at the CASSCF (the complete-active-space SCF) level of calculations, using the Def2-SVP basis set.[86] Starting from the bipyramidal geometry of d^8 $M(CO)_5$, CASSCF optimizations have been executed for the electronic ground state and a few low lying excited states in order to pursue the geometry change. The singlet ground-state configuration complies with a closed shell $(\sigma_{CO/z^2})^2(\pi_{CO/yz})^2(\pi_{CO/xz})^2(3d_{xz})^2(3d_{yz})^2(3d_{xy})^2(3d_{x^2-y^2})^2$ configuration (Fig. 1). Low-lying virtual orbitals conform to $\pi^*_{CO}/3d_{xz}$, $\pi^*_{CO}/3d_{yz}$, $3d_{z^2}/\sigma^*_{CO}$. The minima, crossing minima and transition states are determined using Cartesian coordinates so the computational geometries are independent of any specific choice of internal variables. Each stationary point is executed by its harmonic frequencies, which are computed analytically at the CASSCF(14,10) level of theory.

For better energetic values, the multi-reference Møller–Plesset (MP2-CAS) algorithm[87] is used for electron correlations. Therefore, the relative energies that are obtained in this study are those established at the MP2-CAS(14,10)/Def2-SVP level, using the CASSCF(14,10)/Def2-SVP geometry, which are hereafter designated as MP2-CAS and CASSCF, respectively. The GAUSSIAN 09 package of programs[88] is used for all of the computations. The absolute energies and the Cartesian coordinates for the stationary points are available as ESI.†

III. Results and discussion

(1) The photoactivation reaction for $Fe(CO)_5$

In this section, the photochemical CO-dissociation reaction pathways for iron pentacarbonyl complex $Fe(CO)_5$ (**Fe-S_0-Rea**) is presented since its photochemistry has been extensively studied by many research groups.[2–66,89] A schematic overview of the CO-extrusion mechanism with the relative energies is shown in

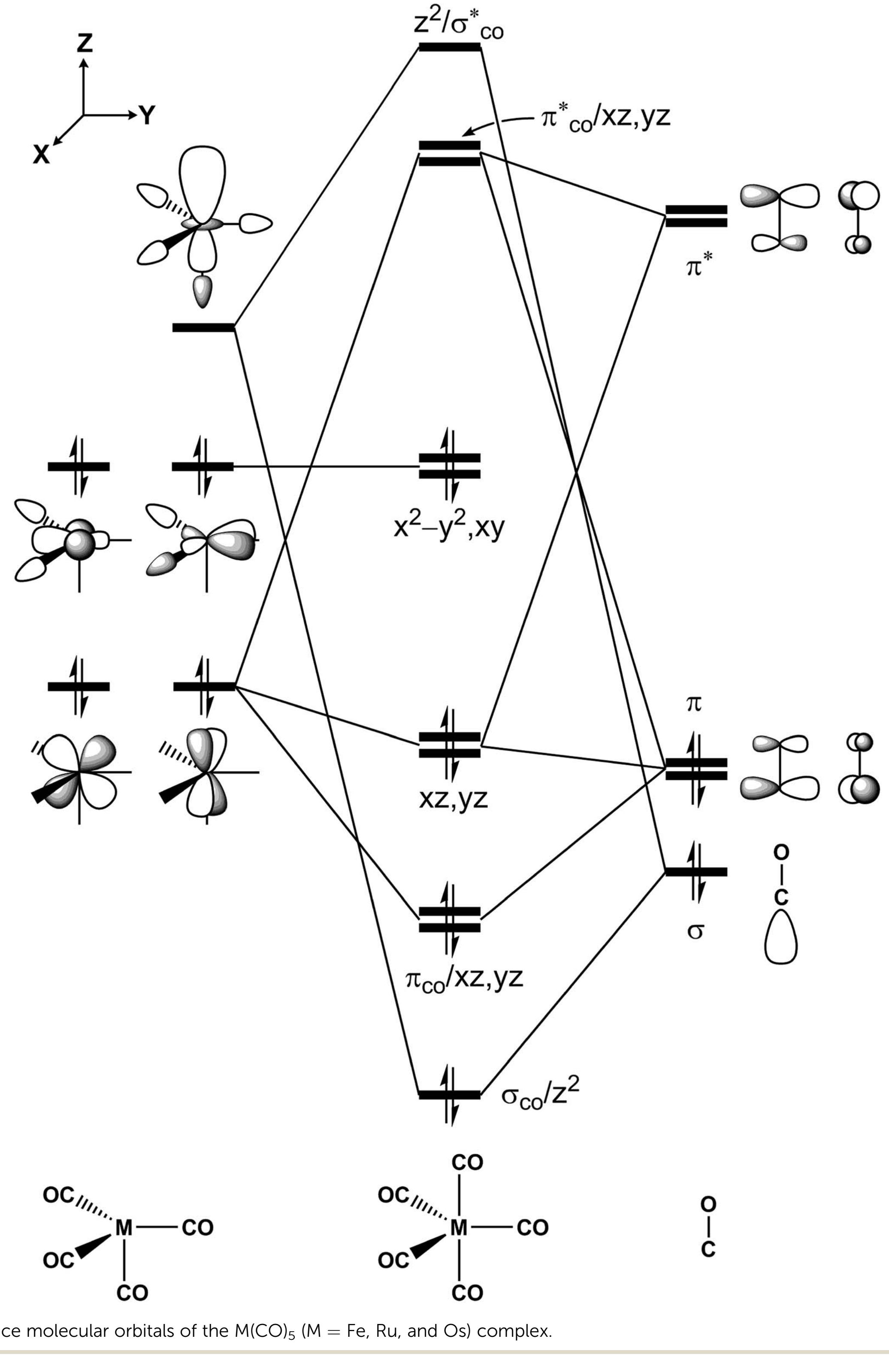

Fig. 1 The valence molecular orbitals of the $M(CO)_5$ (M = Fe, Ru, and Os) complex.

Fig. 2. The corresponding optimized molecular structures are all listed in Fig. 3.

The MP2-CAS//CAS/Def2-SVP computations given in the left-hand side of Fig. 2 demonstrate that the relative energies (kcal mol^{-1}) of the excited Franck–Condon region for $Fe(CO)_5$ increase in the order: **Fe-S_0-Rea** (0.0) < **Fe-T_1-FC** (75.4) < **Fe-T_2-FC** (80.7) < **Fe-S_1-FC** (89.3) < **Fe-T_3-FC** (103.9) < **Fe-S_2-FC** (105.2) < **Fe-T_4-FC** (107.3). It is noted that these MP2-CAS results reveal that the energy of the singlet first excited state (**Fe-S_1-FC**) is higher than those of two triplet excited states (**Fe-T_1-FC** and **Fe-T_2-FC**).

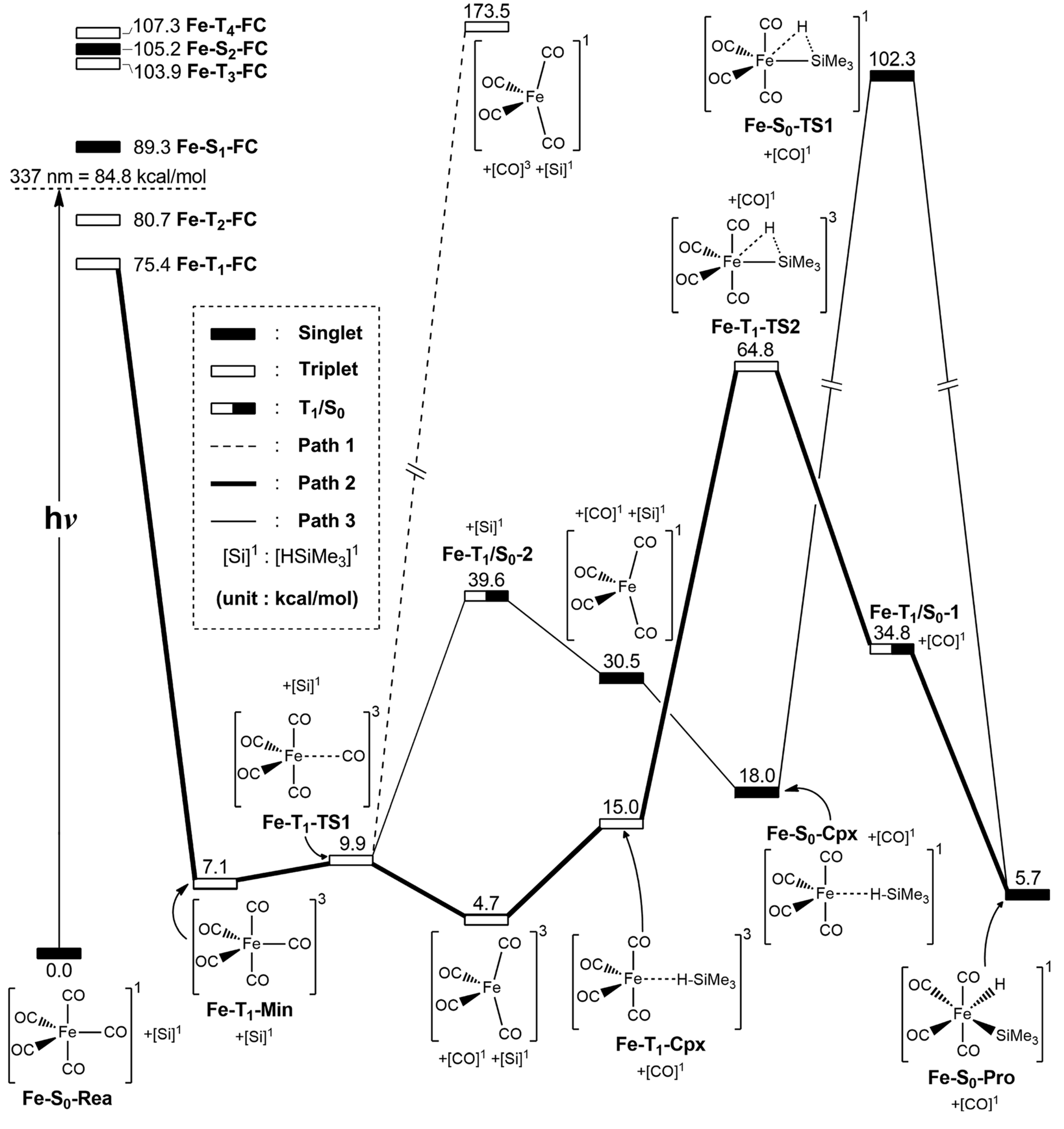

Fig. 2 The potential energy surface based on the MP2-CAS(14,10)/Def2-SVP//CAS(14,10)/Def2-SVP level of theory for the CO-photoextrusion reaction and the oxidative addition reaction mechanisms of Fe(CO)$_5$ (**Fe-S$_0$-Rea**). FC and CI stand for Franck–Condon and conical intersection, respectively. All energies (in kcal mol^{-1}) are given with respect to the reactant (**Fe-S$_0$-Rea**). For the key points of the CASSCF optimized structures, see Fig. 3.

Additionally, the reported experimental absorption band is 337 nm (=84.8 kcal mol^{-1}),[2,15] which is lower in energy than **Fe-S$_1$-FC** by 4.5 kcal mol^{-1}. These evidences strongly suggest that once **Fe-S$_0$-Rea** is photo-irradiated with 337 nm light into an excited electronic state, this species may subsequently relax to the triplet lowest excited state (**Fe-T$_1$-FC**). However, one reviewer pointed out that since the vertical Franck–Condon S$_1$ energy of (**Fe-S$_1$-FC**), which differs with respect to the experimentally observed UV absorption energy, it is could be possible that UV excitation does not purely populate the S$_1$ state, but instead populates a state that involves several configurations, hence the discrepancy in energy value. Nevertheless, our theoretical findings concluded that the photochemical carbonylation reaction of **Fe-S$_0$-Rea** should occur from a triplet first excited state within the FC zone (**Fe-T$_1$-FC**), which agrees satisfactorily with the experimental observations.[2–66]

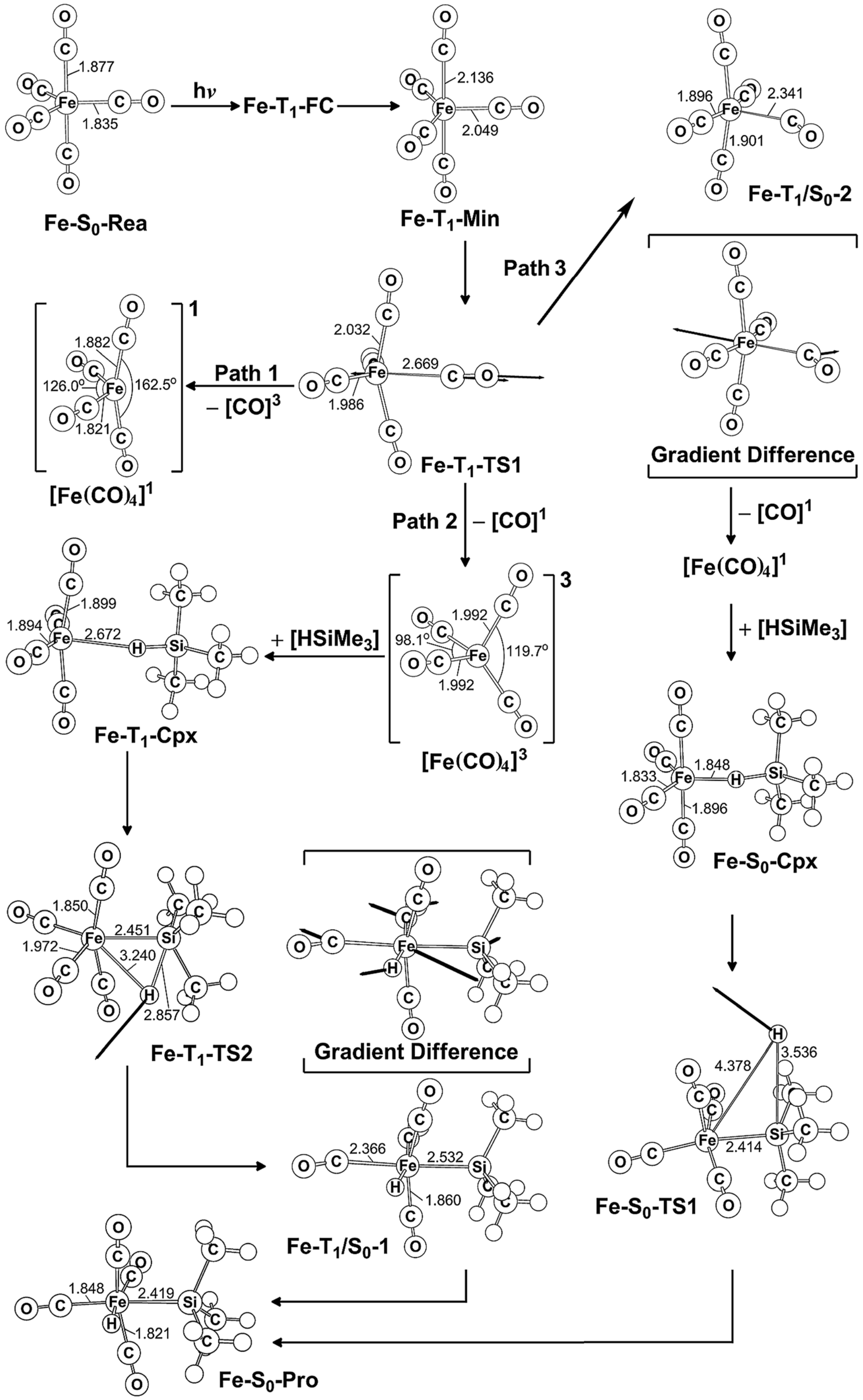

Fig. 3 CAS(14,10)/Def2-SVP optimized geometries (in Å and deg) for the key points of the reactant Fe(CO)$_5$ (**Fe-S$_0$-Rea**) on the potential energy surfaces of paths 1, 2, and 3. The bold arrows indicate the principal atomic motions in the transition state eigenvector. The relative energies for each point are given in Fig. 2. Some hydrogen atoms are omitted for clarity.

As seen in Fig. 2, after irradiation with UV light,[2–66] the reactant (**Fe-S$_0$-Rea**) can relax to a local minimum at the triplet state **Fe-T$_1$-Min**, whose conformation is near to the S$_0$ geometry, as shown in Fig. 3. The MP2-CAS computations show that its energy is calculated to be about 7.1 kcal mol^{-1} greater than **Fe-S$_0$-Rea**, as illustrated in Fig. 2. From **Fe-T$_1$-Min**, a transition state search for the Fe–CO bond breaking, using the geometry of **Fe-T_1-Min**, is undertaken. The optimized structure of **Fe-T_1-TS1** and the calculated transition vector at the CASSCF level are given in Fig. 3. These computations show that this transition state (**Fe-T_1-TS1**) lies only 2.8 kcal mol^{-1} above the **Fe-T_1-Min** point. From the **Fe-T_1-TS1** point, the $Fe(CO)_4$ species then undergoes an oxidative addition reaction with trimethylsilane to yield the final product, **Fe-S_0-Pro**. This gives rise to three types of reaction routes (paths 1, 2, and 3), as shown in Fig. 2.

On path 1, after the **Fe-T_1-TS1** point, the species separates into two molecules with different spin states. One is the $Fe(CO)_4$ molecule in the singlet state, which is denoted **$[Fe(CO)_4]^1$**, and the other is the CO molecule at the triplet excited state, which is denoted $[CO]^3$. The MP2-CAS computations show that the energies of **$[Fe(CO)_4]^1$** and $[CO]^3$ are 174 kcal mol^{-1} higher than that of the corresponding reactant (**Fe-S_0-Rea**). Since this relative energy much higher than the available experimental observations for UV irradiation,[2,54–66] it is not possible to generate both products (**$[Fe(CO)_4]^1$** and $[CO]^3$). Therefore, path 1 is unlikely because of the high activation energy that is required. The computations indicate that the reaction mechanism for path 1 is as follows: ($[Si]^1$ acts for trimethylsilane in the singlet state.)

Path 1: **Fe-S_0-Rea** + $[Si]^1$ + *hν* → **Fe-T_1-Min** + $[Si]^1$ → **Fe-T_1-TS1** + $[Si]^1$ → **$[Fe(CO)_4]^1$** + $[CO]^3$ + $[Si]^1$

On path 2, after the **Fe-T_1-TS1** point, the species divides into two fragments: one triplet intermediate **$[Fe(CO)_4]^3$** and one singlet CO molecule. The **$[Fe(CO)_4]^3$** then interacts with trimethylsilane to yield the triplet precursor complex (**Fe-T_1-Cpx**), which is estimated to be 15.0 kcal mol^{-1} above the corresponding reactants. Fortunately, the activation barrier from **Fe-T_1-Cpx** to **Fe-T_1-TS2** is calculated to be 49.8 kcal mol^{-1}, which is much greater than the complex energy (15.0 kcal mol^{-1}), so **Fe-T_1-Cpx** should be readily observed in experiments. The Si–H bond-breaks *via* the triplet **Fe-T_1-TS2**, and then this species loosens to produce the final insertion product (**Fe-S_0-Pro**) across the intersystem crossing point (**Fe-T_1/S_0-1**). Because the activation energy (49.8 kcal mol^{-1}) for path 2 is computed to be much less than the reported energy of the UV irradiation,[2,15–28] path 2 should be energetically accessible. Consequently, the mechanism for path 2 is as follows:

Path 2: **Fe-S_0-Rea** + $[Si]^1$ + *hν* → **Fe-T_1-Min** + $[Si]^1$ → **Fe-T_1-TS1** + $[Si]^1$ → **$[Fe(CO)_4]^3$** + $[CO]^1$ + $[Si]^1$ → **Fe-T_1-Cpx** + $[CO]^1$ → **Fe-T_1-TS2** + $[CO]^1$ → **Fe-T_1/S_0-1** + $[CO]^1$ → **Fe-S_0-Pro** + $[CO]^1$

On path 3, many experimental observations[2,15–28] show that the photochemical loss of a CO ligand from the $Fe(CO)_5$ molecule results in the formation of the triplet **$[Fe(CO)_4]^3$** intermediate and then proceeds ultimately along the singlet ground state path. This strongly implies that the crossing point for the triplet and singlet surfaces plays a central role in describing the mechanistic CO-photoelimination reaction for **Fe-S_0-Rea**. Therefore, intersystem crossing from triplet to singlet states occurs in the region of the T_1/S_0 intersection **Fe-T_1/S_0-2**, as given in Fig. 2. These MP2-CAS calculations predict that **Fe-T_1/S_0-2** lies 39.6 kcal mol^{-1} above **Fe-S_0-Rea**. This molecule then relaxes to a singlet **$[Fe(CO)_4]^1$** intermediate and one singlet CO molecule, whose relative energy is computed to be 30.5 kcal mol^{-1}, with respect to **Fe-S_0-Rea**. **$[Fe(CO)_4]^1$** then reacts with trimethylsilane to generate a singlet precursor complex (**Fe-S_0-Cpx**), which is computed to be 18.0 kcal mol^{-1} higher in energy than the initial reactants. This precursor complex then undergoes an insertion process to reach the transition state **Fe-S_0-TS1**, initially *via* a Si–H bond stretching with a hydrogen migrating to the iron center, as shown in Fig. 3. Fig. 2 demonstrates that the activation barrier from **Fe-S_0-Cpx** to **Fe-S_0-TS1** is calculated to be 84.3 kcal mol^{-1}. This theoretical evidence strongly suggests that it is difficult for the precursor complex (**Fe-S_0-Cpx**) to override barrier since this barrier is too high to be reached to the final insertion product (**Fe-S_0-Pro**). It is, therefore, predicted that **Fe-S_0-Cpx** could be easily detected experimentally. Indeed, this theoretical prediction has been confirmed by several experimental observations.[29–32]

Based on these theoretical calculations, the mechanism for path 3 is as follows:

Path 3: **Fe-S_0-Rea** + $[Si]^1$ + *hν* → **Fe-T_1-Min** + $[Si]^1$ → **Fe-T_1-TS1** + $[Si]^1$ → **Fe-T_1/S_0-2**+ $[Si]^1$ → **$[Fe(CO)_4]^1$** + $[CO]^1$ + $[Si]^1$→ **Fe-T_1/S_0-3** + $[CO]^1$ + $[Si]^1$→ **$[Fe(CO)_4]^3$** + $[CO]^1$ + $[Si]^1$ → **Fe-T_1-Cpx** + $[CO]^1$ → **Fe-T_1-TS2** + $[CO]^1$ → **Fe-T_1/S_0-1**+ $[CO]^1$ → **Fe-S_0-Pro** + $[CO]^1$

In brief, these theoretical computations show that under irradiation by UV light, $Fe(CO)_5$ (**Fe-S_0-Rea**) generates a coordinately unsaturated 16-electron tetracarbonyl iron (0) intermediate that exists in either the singlet or the triplet states by way of the photochemical loss of one CO ligand. After this CO-photodissociation, the dynamic $Fe(CO)_4$ species readily experiences oxidative addition of an Si–H bond to an iron center to produce an insertion product. These model studies show there are three possible reaction pathways (path 1, path 2, and path 3) for the photo-assisted Si–H bond activation reaction. Only path 2 is shown to be energetically favorable reaction route for the alkylsilane oxidative addition reactions because this reaction pathway allows the production of the $Fe(CO)_4$ fragment at the triplet ground state, but the other routes (path 1 and path 3) generate the singlet excited $Fe(CO)_4$ intermediate. In other words, these model observations demonstrate that the singlet excited tetracarbonyl iron (0) plays no role in the photochemical oxidative addition reactions of alkylsilanes. However, the singlet excited $Fe(CO)_4$ moiety interacts with alkylsilane to yield a singlet van der Waal's complex (**Fe-S_0-Cpx**), which is readily experimentally detectable. Because of the moderate barrier height for the triplet **Fe-T_1-Cpx** species, as shown in Fig. 2, this triplet van der Waal's complex should also be experimentally observable.[11–37,48–79]

(2) The photoactivation reaction for $Ru(CO)_5$

The co-photoextrusion and the oxidative addition reaction mechanisms of the pentacarbonyl complex that contains the next transition metal element in the group 8 family, $Ru(CO)_5$ (**Ru-S$_0$-Rea**), is examined. Since previous several theoretical studies[38,39,43–45] have demonstrated that the ground state of the $Ru(CO)_4$ fragment favors a low-spin electronic ground state and its calculated triplet–singlet energy splitting ($=E_{\text{triplet}} - E_{\text{singlet}}$) is about 13.1–25.0 kcal mol^{-1} at different levels of theory, the conical intersection pathway is used to study the CO-photodissociation mechanism of **Ru-S$_0$-Rea**. A sketch of the potential energy surfaces for the reaction routes that lead to the CO dissociation and the Si–H bond oxidative addition reactions is shown in Fig. 4. The calculated geometrical structures for specific parameters at the CASSCF level of theory are all shown in Fig. 5.

Initially, the reactant (**Ru-S$_0$-Rea**) is promoted to the singlet excited state by way of a vertical excitation (**Ru-S$_1$-FC**), as shown on the left-hand side of Fig. 4. It is noted that the calculated vertical singlet excitation energy at the MP2-CAS level of theory (110.7 kcal mol^{-1}) agrees with the available experimental results. Bogdan and Weitz reported that the unsaturated 16 electron $Ru(CO)_4$ is a photoproduct of the irradiation of $Ru(CO)_5$ by 248 nm (=115.3 kcal mol^{-1}) radiation.[45] As mentioned previously, the theoretical calculations show that the $Ru(CO)_4$ fragment should have a singlet electronic ground state.[38,39,43,46,47] These results show that the only excited state that is involved in the photochemical carbonyl elimination reaction for $Ru(CO)_5$ (**Ru-S$_0$-Rea**) is the singlet.

From the Franck–Condon point (**Ru-S$_1$-FC**), the species relaxes to a conical intersection (**Ru-S$_1$/S$_0$-CI**) between the singlet excited- and ground-electronic states. As seen in Fig. 5, funneling through the **Ru-S$_1$/S$_0$-CI** point results in two different reaction routes on the ground state surface, *via* either the derivative coupling vector or the gradient difference vector.[80–85] The derivative coupling vector for **Ru-S$_1$/S$_0$-CI** is almost an antisymmetric bending motion, which produces a vibrationally hot species in the singlet ground-state configuration. Its gradient difference vector produces one equatorial Ru–CO bond breaking. Therefore, following the gradient difference vector from **Ru-S$_1$/S$_0$-CI** and dissociating one equatorial Ru–CO bond leads to a ruthenium complex with tetracarbonyls (**Ru-S$_0$-Int**) and one CO molecule. The MP2-CAS calculations show that the energy of **Ru-S$_1$/S$_0$-CI**, relative to the initial reactant (**Ru-S$_0$-Rea**), is 45.4 kcal mol^{-1}, but it is 71.7 kcal mol^{-1} lower than **Ru-S$_1$-FC**. In other words, beginning from the **Ru-S$_1$-FC** point, $Ru(CO)_5$ enters an efficacious decay tunnel (**Ru-S$_1$/S$_0$-CI**). From this conical intersection, the 16-electron photoproduct (**Ru-S$_0$-Int**) and the initial reactant (**Ru-S$_0$-Rea**) are readily obtained *via* a barrierless ground-state relaxation path.

The unsaturated $Ru(CO)_4$ species then reacts with trimethylsilane to form a precursor complex (**Ru-S$_0$-Cpx**) at the singlet ground state. Subsequently, one hydrogen migrates from the silicon atom to the ruthenium center *via* a transition state (**Ru-S$_0$-TS1**). The insertion product (**Ru-S$_0$-Pro**) is then produced. The barrier energy from **Ru-S$_0$-Cpx** to **Ru-S$_0$-TS1** is computed to be 63.3 kcal mol^{-1} but the MP2-CAS computations show that the energy of **Ru-S$_1$/S$_0$-CI** lies 71.7 kcal mol^{-1} below that of **Ru-S$_1$-FC**. This evidence shows that the large excess energy of 72 kcal mol^{-1} that is a result of the relaxation from **Ru-S$_1$-FC** to **Ru-S$_1$/S$_0$-CI** is the driving force for further oxidative addition reactions with alkylsilane on the ground state surface. These theoretical findings demonstrate that the photochemical reaction for $Ru(CO)_5$ is as follows:

$Ru(CO)_5$ (photo): **Ru-S$_0$-Rea** + $[Si]^1$ + $h\nu$ → **Ru-S$_1$-FC** + $[Si]^1$ → **Ru-S$_1$/S$_0$-CI** + $[Si]^1$ → **Ru-S$_0$-Int** + $[CO]^1$ + $[Si]^1$ → **Ru-S$_0$-Cpx** + $[CO]^1$ → **Ru-S$_0$-TS1** + $[CO]^1$ → **Ru-S$_0$-Pro** + $[CO]^1$

The thermal (dark) reaction of $Ru(CO)_5$ (**Ru-S$_0$-Rea**) is also examined. As shown in Fig. 4, the energy of $Ru(CO)_4$ (**Ru-S$_0$-Int**) and one CO molecule is calculated to be 36.2 kcal mol^{-1} above that of the corresponding reactant (**Ru-S$_0$-Rea**). Close to the conical intersection region (**Ru-S$_1$/S$_0$-CI**), a CO-thermal-dissociation transition state (**Ru-S$_0$-TS2**) lies on the singlet ground state surface, whose energy is only 5.3 kcal mol^{-1} below that of **Ru-S$_1$/S$_0$-CI**, as shown in Fig. 4. That is to say, the computations predict that the activation energy from **Ru-S$_0$-Rea** to **Ru-S$_0$-TS2** is 40.1 kcal mol^{-1}, but the barrier height from **Ru-S$_0$-Int** to **Ru-S$_0$-TS2** is only 3.9 kcal mol^{-1}. This theoretical evidence strongly suggests that $Ru(CO)_4$ and CO recombine to regenerate the singlet reactant, $Ru(CO)_5$, and that this process is very fast. This theoretical result is in agreement with the available experimental observations.[12,45] According to some experimental reports,[12,45] the singlet $Ru(CO)_4$ fragment i generated during the irradiation of $Ru(CO)_5$, but this ruthenium tetracarbonyl also instantly recombines with CO to form the parent molecule. This is in sharp contrast to the case of $Fe(CO)_5$, as shown in Fig. 2,[11–14] where the photochemical combination of a CO ligand occurs on a potential energy surface with a different spin multiplicity, as discussed in the previous section.

(3) The photoactivation reaction for $Os(CO)_5$

The photochemical reaction mechanisms of the third member of the group 8 triad, $Os(CO)_5$, are reported. Since the $Os(CO)_4$ fragment is known to have the ground-state singlet electronic state, as demonstrated by several experimental[47] and theoretical[39,44] studies, the CO-photodissociation mechanism for $Os(CO)_5$ (**Os-S$_0$-Rea**) from the conical intersection mechanism viewpoints is studied. Fig. 6 shows the potential energy surface for the reaction pathways that give rise to the CO dissociation and the Si–H bond oxidative addition reaction with trimethylsilane. Fig. 7 also shows the CASSCF/Def2-SVP computed structures with some key geometrical parameters.

Similarly to $Ru(CO)_5$ as shown in Fig. 4, Fig. 6 shows that the irradiation of $Os(CO)_5$ with light promotes it to the singlet first excited state in the Franck–Condon region, (**Os-S$_1$-FC**). Calculations at the MP2-CAS level of theory show reveal the promotion energy for **Os-S$_0$-Rea** is estimated to be 113.7 kcal mol^{-1}. This theoretical value is in good agreement with the reported experimental data (248 nm = 115.3 kcal mol^{-1}).[47] This agreement means that the subsequent computational results for the photochemical reaction for $Os(CO)_5$ are reliable.

The photoexcited $Os(CO)_5$ undergoes radiation-less relaxation to the singlet ground state surface through the conical intersection point, (**Os-S$_1$/S$_0$-CI**), whose geometrical structure is

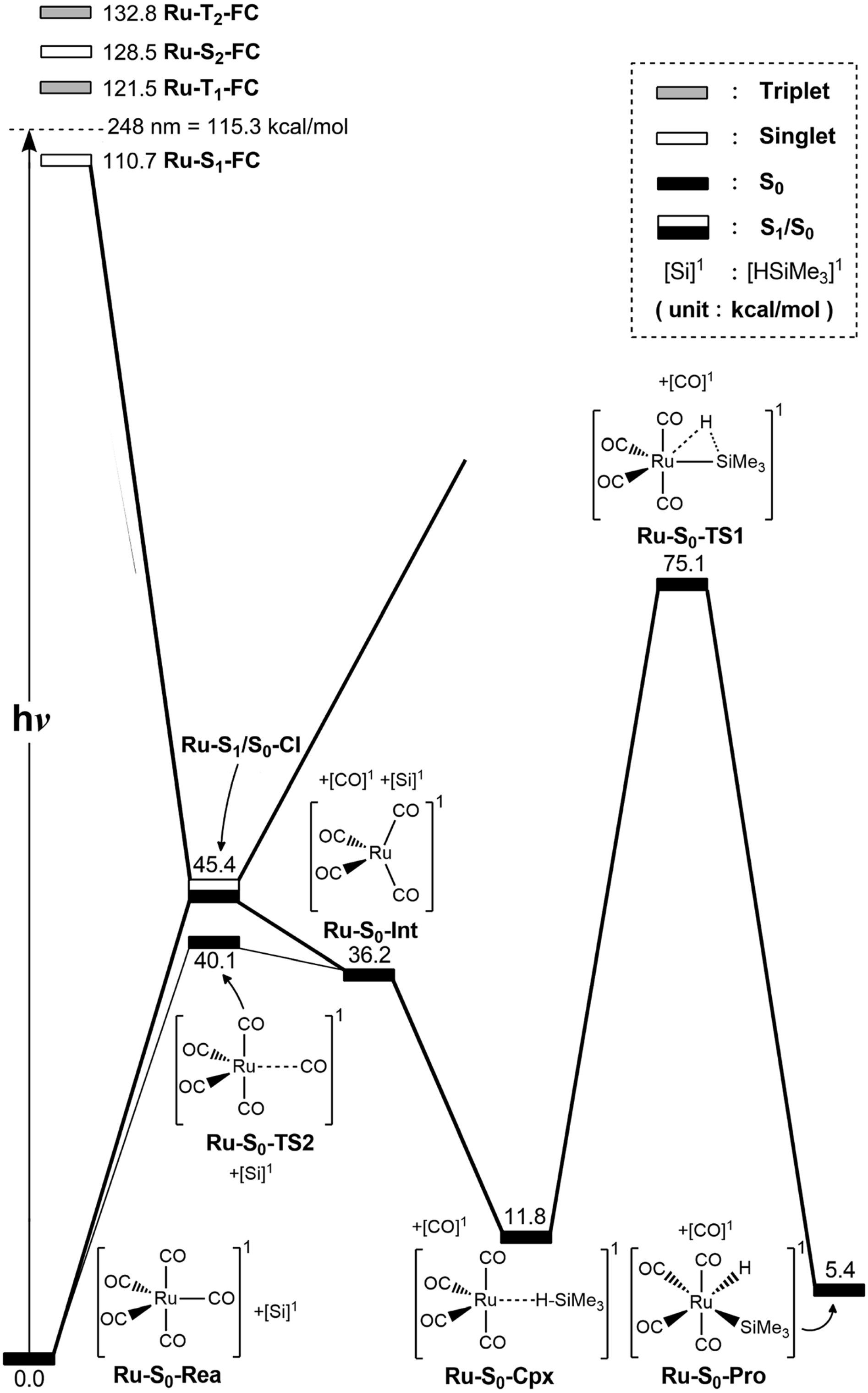

Fig. 4 The potential energy surface based on the MP2-CAS(14,10)/Def2-SVP//CAS(14,10)/Def2-SVP level of theory for the CO-photoextrusion reaction and the oxidative addition reaction mechanisms of Ru(CO)$_5$ (**Ru-S$_0$-Rea**). FC and CI stand for Franck–Condon and conical intersection, respectively. All energies (in kcal mol^{-1}) are given with respect to the reactant (**Ru-S$_0$-Rea**). For the key points of the CASSCF optimized structures, see Fig. 5.

shown in Fig. 7. Previous experience of the CO photoelimination mechanism for Ru(CO)$_5$ shows that the breaking of an equatorial Os–CO bond plays a central role in the photoextrusion reaction for **Os-S$_0$-Rea.** Indeed, along the Os–CO stretching reaction path, **Os-S$_1$/S$_0$-CI** is acquired at the Os–CO bond length of 3.697 Å. The MP2-CAS results show that the

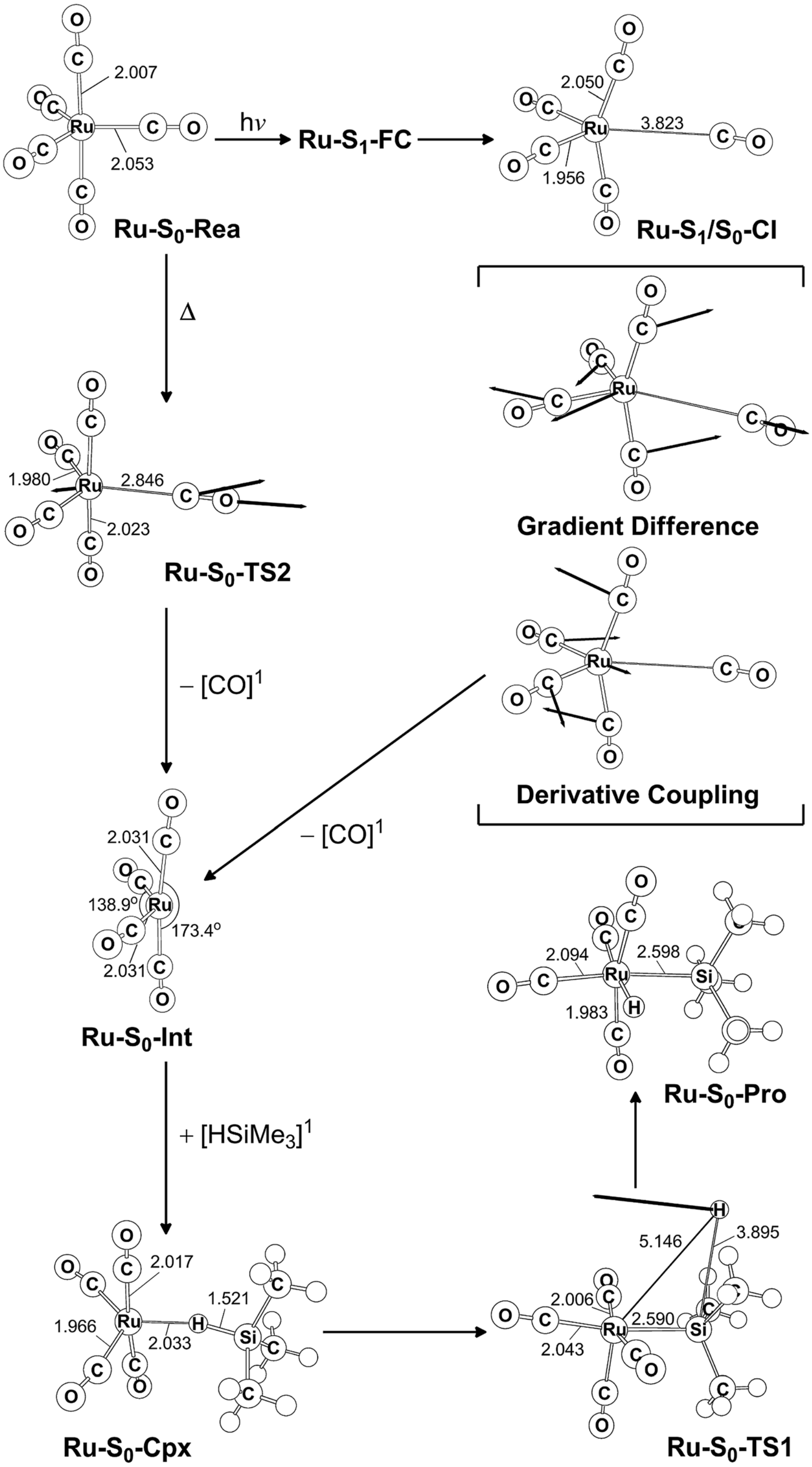

Fig. 5 CAS(14,10)/Def2-SVP optimized geometries (in Å and deg) for the key points for the reactant, Ru(CO)$_5$ (**Ru-S$_0$-Rea**), on the potential energy surfaces. The bold arrows indicate the principal atomic motions in the transition state eigenvector. The relative energies for each species are shown in Fig. 4. Some hydrogen atoms are omitted for clarity.

energy of **Os-S$_1$/S$_0$-CI** lies 57.1 kcal mol^{-1} above the initial reactant, but 63.2 kcal mol^{-1} below **Os-S$_1$-FC.** This species then decays to an Os(CO)$_4$ fragment (**Os-S$_0$-Int**) and one CO molecule. The computational data that is shown in Fig. 6 shows that the large excess energy of 74.6 kcal mol^{-1} that results from the relaxation from **Os-S$_1$-FC** to **Os-S$_0$-Int** is the driving force for a further oxidative addition reaction with alkylsilane on the singlet ground state surface (see below).

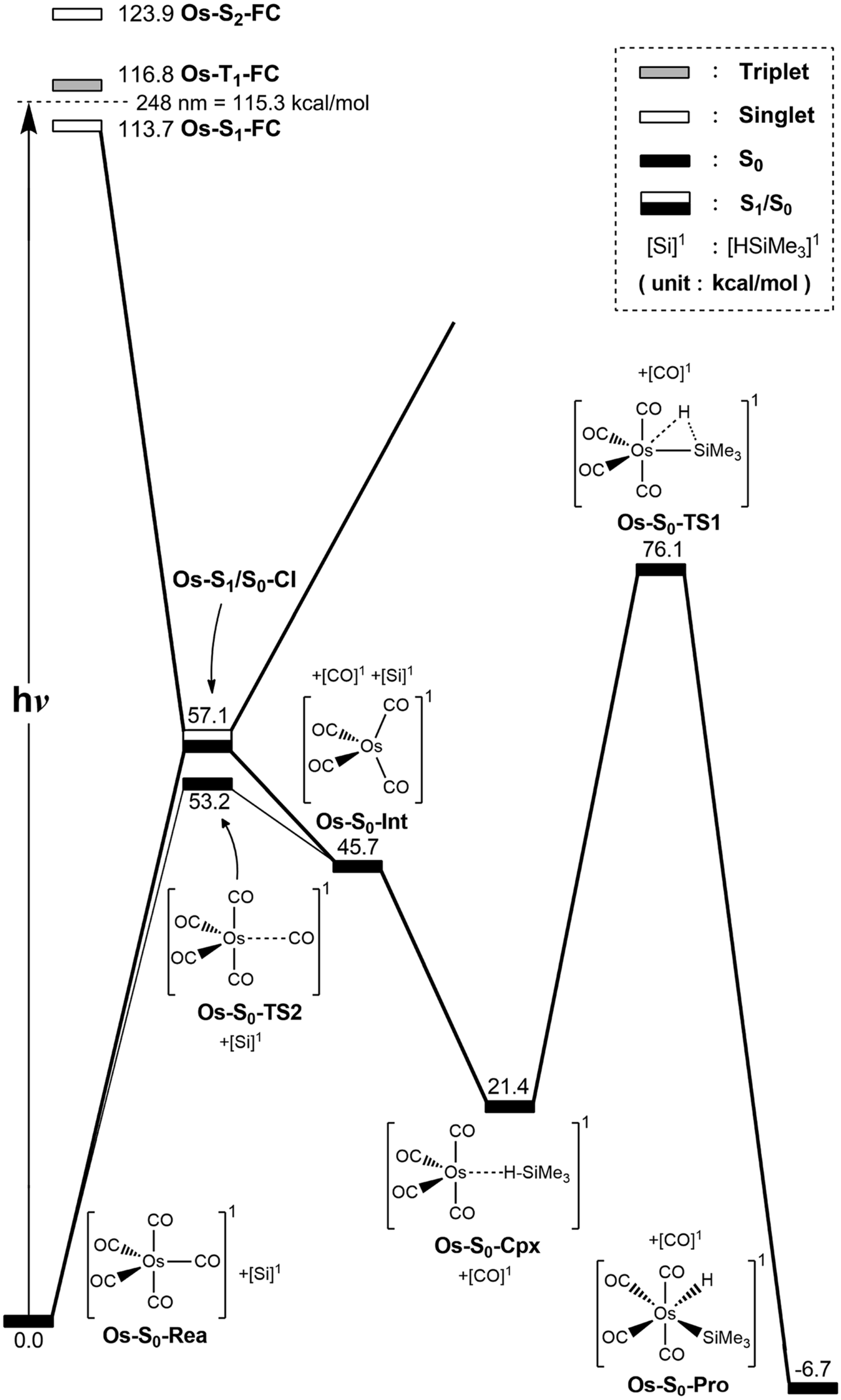

Fig. 6 The potential energy surface based on the MP2-CAS(14,10)/Def2-SVP//CAS(14,10)/Def2-SVP level of theory for the CO-photoextrusion reaction and the oxidative addition reaction mechanisms of $Os(CO)_5$ (**Os-S$_0$-Rea**). FC and CI stand for Franck–Condon and conical intersection, respectively. All energies (in kcal mol^{-1}) are given with respect to the reactant (**Os-S$_0$-Rea**). For the key points of the CASSCF optimized structures, see Fig. 7.

This unsaturated 16-electron **Os-S$_0$-Int** fragment also reacts with trimethylsilane to form the initial precursor complex, **Os-S$_0$-Cpx,** whose energy is computed to be 21.4 kcal mol^{-1}, relative to parent molecules. The species then undergoes a 1,2-hydrogen shift *via* a transition state (**Os-S$_0$-TS1**) to yield the final insertion product (**Os-S$_0$-Pro**). Because of the large excess

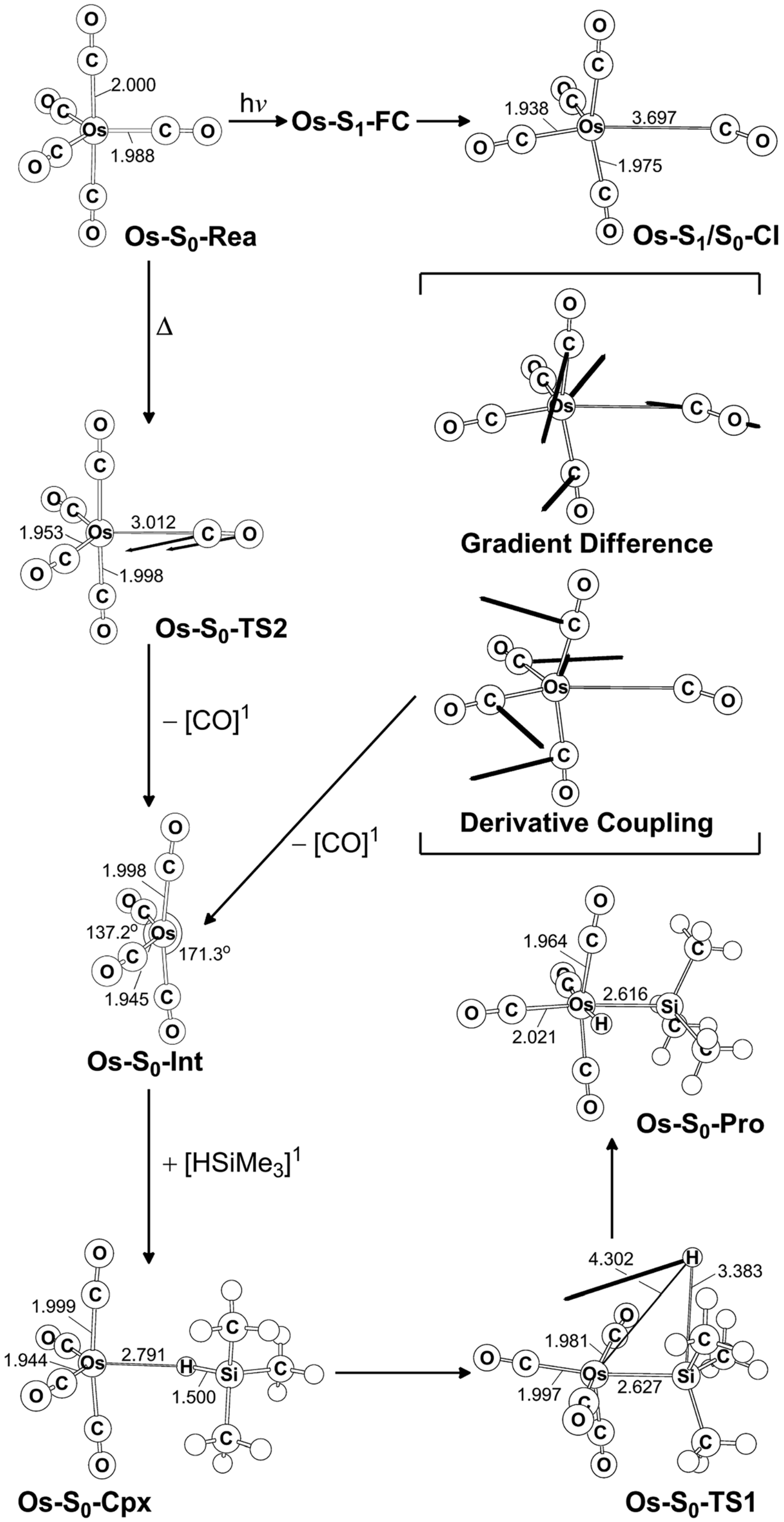

Fig. 7 CAS(14,10)/Def2-SVP optimized geometries (in Å and deg) for the critical points for the reactant, $Os(CO)_5$ (**Os-S_0-Rea**), on the potential energy surfaces. The bold arrows indicate the principal atomic motions in the transition state eigenvector. The relative energies for each species are shown in Fig. 6. Some hydrogen atoms are omitted for clarity.

energy (74.6 kcal mol^{-1}) mentioned previously, the species readily overcomes the barrier (54.7 kcal mol^{-1}) from **Os-S_0-Cpx** to **Os-S_0-TS1.** The theoretical findings show that similarly to the photochemical mechanism for $Ru(CO)_5$ studied earlier, $Os(CO)_5$ proceeds along the following photochemical reaction pathway:

$$\text{Os(CO)}_5\ \text{(photo)}: \textbf{Os-S}_0\textbf{-Rea} + [\text{Si}]^1 + h\nu \rightarrow \textbf{Os-S}_1\textbf{-FC} + [\text{Si}]^1 \rightarrow \textbf{Os-S}_1\textbf{/S}_0\textbf{-CI} + [\text{Si}]^1 \rightarrow \textbf{Os-S}_0\textbf{-Int} + [\text{CO}]^1 + [\text{Si}]^1 \rightarrow \textbf{Os-S}_0\textbf{-Cpx} + [\text{CO}]^1 \rightarrow \textbf{Os-S}_0\textbf{-TS1} + [\text{CO}]^1 \rightarrow \textbf{Os-S}_0\textbf{-Pro} + [\text{CO}]^1$$

The thermal (dark) reaction mechanism for $Os(CO)_5$ is also examined using the same level of theory. As is seen in Fig. 6, the MP2-CAS results show that the energies for **Os-S$_0$-TS2**, and **Os-S$_0$-Int** + $[CO]^1$ are respectively calculated to be 53.2 and 45.7 kcal mol^{-1}, with respect to the corresponding reactant. In other words, the reverse barrier height from **Os-S$_0$-Int** + $[CO]^1$ to **Os-S$_0$-TS2** is estimated to be 7.5 kcal mol^{-1}. This theoretical finding shows that the unsaturated $Os(CO)_4$ fragment easily recombines with one CO molecule to return to the parent molecule, $Os(CO)_5$. In other words, this theoretical study shows that the reactivity of the unsaturated $Os(CO)_4$ complex is quite similar to that of the analogous $Ru(CO)_4$ compound.[12,46,47]

IV. Conclusion

The photochemical reaction mechanisms for the CO dissociation and the related oxidative addition with alkylsilane for group 8 metal pentacarbonyl complexes are studied. Taking the group 8 triad systems together, the following conclusions can be drawn:

These computational results are in good agreement with the formation of an intermediate of a metal tetracarbonyl fragment (d^8 $M(CO)_4$) by the photochemical loss of one CO ligand from the parent molecule (d^8 $M(CO)_5$), which is in good agreement with many experimental findings.[2–79]

For the $Fe(CO)_5$ model molecule, the theoretical findings show that the singlet–triplet energy difference of $Fe(CO)_4$ is calculated to be 25.8 kcal mol^{-1} (MP2-CAS/Def2-SVP//CASSCF/Def2-SVP) and it has a triplet electronic ground state.[90] Knowledge of the intersystem crossing mechanism for the $Fe(CO)_5$ complex is of great importance in understanding its reaction mechanisms because it is the driving force for photochemistry. The theoretical evidence shows that the triplet iron tetracarbonyl activates the Si–H bond of alkylsilane much more readily than its singlet counterpart.

However, these theoretical results show that it is difficult for the CO molecule to recombine with the $Fe(CO)_4$ complex, which has a vacant coordination site because the iron tetracarbonyl is proven to have a triplet electronic ground state but CO has a singlet ground state. Therefore, according to spin selection rules, it should be difficult for the triplet $Fe(CO)_4$ and the singlet CO to recombine to generate the parent $Fe(CO)_5$ molecule. This theoretical observation is in good agreement with many experimental results.[2,11–25,33–37]

For the $Ru(CO)_5$ and $Os(CO)_5$ model compounds, both ruthenium and osmium pentacarbonyls have similar photochemical and thermal potential energy profiles. The computations also show that both $Ru(CO)_4$ and $Os(CO)_4$ fragments feature a singlet electronic ground state. Therefore, the computations demonstrate that the conical intersection mechanism plays a vital role in the photochemical reactions for the $Ru(CO)_5$ and $Os(CO)_5$ transition metal complexes. The theoretical observations also show that the activation barrier for the thermal fragmentation reactions for Ru and Os pentacarbonyls are much higher than those for the thermal recombination reactions for the corresponding $M(CO)_4$ fragments and CO. Therefore, after the loss of CO from $Ru(CO)_5$ or $Os(CO)_5$, the CO molecule readily recombines with $Ru(CO)_4$ or $Os(CO)_4$ to form the parent compounds. This finding is in agreement with several experimental observations.[11–25,38–47]

This theoretical evidence demonstrates that $Fe(CO)_5$ readily undergoes one CO ligand dissociation upon irradiation with light to form the very reactive unsaturated intermediate $Fe(CO)_4$ species, but it is difficult for either $Ru(CO)_5$ or $Os(CO)_5$ to dissociate one CO group. Therefore, the yield of oxidative addition product for the $Fe(CO)_5$ molecule should be much larger than those for the $Ru(CO)_5$ and $Os(CO)_5$ systems, for the same reactive conditions.

The photochemistry of d^8 $M(CO)_5$ is salient to many types of photochemical reaction. The subtle variation poses a mechanistic challenge and it is hoped that this study will stimulate further study of this subject.

Conflicts of interest

There are no conflicts to declare.

Acknowledgements

The authors are grateful to the National Center for High-Performance Computing of Taiwan for generous amounts of computing time, and the Ministry of Science and Technology of Taiwan for the financial support. In particular, one of the authors (M.-D. Su) also wishes to thank Professor Michael A. Robb, Dr S. Wilsey, Dr Michael J. Bearpark, (University of London, UK) and Professor Massimo Olivucci (Universita degli Studi di Siena, Italy), for their encouragement and support during his stay in London. Special thanks are also due to reviewers 1, 2, and 3 for very helpful suggestions and comments.

References

1 For reviews, see: M. Warighton, Photochemistry of metal carbonyl, *Chem. Rev.*, 1974, **74**, 401.

2 For reviews, see: N. Leadbeater, Enlightening organometallic chemistry: the photochemistry of $Fe(CO)_5$ and the reaction chemistry of unsaturated iron carbonyl fragments, *Coord. Chem. Rev.*, 1999, **188**, 35.

3 F. W. Grevels, in *Photoprocesses in Transition Metal Complexes, Biosystems and Other Molecules*, ed. E. Kochanski, Kluwer, Amsterdam, 1992.

4 G. L. Geoffroy and M. S. Wrighton, in *Organometallic Photochemistry*, Academic Press, New York, 1979.

5 V. Balzani and V. Carassiti, in *Photochemistry of Coordination Compounds*, Academic Press, London, 1970.

6 A. Marquez, C. Daniel and J. F. Sanz, The vacuum-ultraviolet spectrum of iron pentacarbonyl: an experimental analysis

supported by a CASSCF CCI study of the Rydberg states, *J. Phys. Chem.*, 1992, **96**, 121.

7 F. Asinger and O. Berg, Über die Isomerisierung der olefinischen Doppelbindung durch Metallcarbonyle, *Chem. Ber.*, 1955, **88**, 445.

8 E. N. Frankel, E. A. Emken, H. M. Peters, V. L. Davison and R. O. Butterfield, Homogeneous Hydrogenation of Methyl Linoleate Catalyzed by Iron Pentacarbonyl. Characterization of Methyl Octadecadienoate—Iron Tricarbonyl Complexes, *J. Org. Chem.*, 1964, **29**, 3292.

9 F. K. Velichko and L. V. Vinogradova, *Izv. Akad. Nauk SSSR, Ser. Khim.*, 1970, 1628.

10 M. S. Sigman and B. E. Eaton, Catalytic Iron-Mediated [4 + 1] Cycloaddition of Diallenes with Carbon Monoxide, *J. Am. Chem. Soc.*, 1996, **118**, 11783.

11 M. Poliakoff, II $Fe(CO)_4$, *Chem. Soc. Rev.*, 1978, 527.

12 M. Poliakoff and E. Weitz, Shedding light on organometallic reactions: the characterization of tetracarbonyliron ($Fe(CO)_4$), a prototypical reaction intermediate, *Acc. Chem. Res.*, 1987, **20**, 408.

13 M. Poliakoff, S. M. Howdle and S. G. Kazarian, Vibrational Spectroscopy in Supercritical Fluids: From Analysis and Hydrogen Bonding to Polymers and Synthesis, *Angew. Chem., Int. Ed.*, 1995, **34**, 12751.

14 J. P. Lomont, S. C. Nguyen and C. B. Harris, Ultrafast Infrared Studies of the Role of Spin States in Organometallic Reaction Dynamics, *Acc. Chem. Res.*, 2014, **47**, 1634.

15 A. B. Callear and R. J. Oldman, Absorption Spectra of Excited Atoms and Excited Ions produced by Isothermal Flash Photolysis of Metal Carbonyls in the Gas Phase, *Nature*, 1966, **210**, 730.

16 M. Poliakoff and J. J. Turner, Reactions of organodigermanes, *J. Chem. Soc., Dalton Trans.*, 1973, 1357.

17 M. Poliakoff, Infrared spectrum of matrix isolated tricarbonyliron, *J. Chem. Soc., Dalton Trans.*, 1974, 210.

18 M. Poliakoff and J. J. Turner, Structure and reactions of matrix-isolated tetracarbonyliron(0), *J. Chem. Soc., Dalton Trans.*, 1974, 2276.

19 M. Poliakoff and J. J. Turner, A new route to matrix isolated iron atoms, *J. Chem. Soc., Faraday Trans. 2*, 1974, **70**, 93.

20 T. J. Barton, R. Grinter, A. J. Thomson, B. Davies and M. Poliakoff, Magnetic circular dichroism evidence for the paramagnetism of tetracarbonyliron(0): low-temperature matrix studies, *J. Chem. Soc., Chem. Commun.*, 1977, 841.

21 Z. Karny, R. Naaman and R. N. Zare, Production of excited metal atoms by UV multiphoton dissociation of metal alkyl and metal carbonyl compounds, *Chem. Phys. Lett.*, 1978, **59**, 33.

22 G. Nathanson, B. Gitlin, A. M. Rosan and J. T. Yardley, Ultraviolet laser photolysis: primary photochemistry of $Fe(CO)_5$ in PF_3, *J. Chem. Phys.*, 1981, **74**, 361.

23 M. Poliakoff and J. J. Turner, The Structure of $[Fe(CO)_4]$—An Important New Chapter in a Long-Running Story, *Angew. Chem., Int. Ed.*, 2001, **40**, 2809.

24 M. Poliakoff, The infra-red laser-induced photochemistry of $Fe(CO)_4$, *Spectrochim. Acta*, 1987, **43A**, 217.

25 H. Ihee, J. Cao and A. H. Zewail, Ultrafast Electron Diffraction of Transient $[Fe(CO)_4]$: Determination of Molecular Structure and Reaction Pathway, *Angew. Chem., Int. Ed.*, 2001, **40**, 1532.

26 J. C. Mitchener and M. S. Wrighton, Photogeneration of very active homogeneous catalysts using laser light excitation of iron carbonyl precursors, *J. Am. Chem. Soc.*, 1981, **103**, 975.

27 J. C. Mitchener and M. S. Wrighton, Low-temperature photochemistry of tetracarbonylethyleneiron and tetracarbonylpropyleneiron. Spectroscopic observation of catalytically significant intermediates, *J. Am. Chem. Soc.*, 1983, **105**, 1065.

28 M. Bergt, T. Brixner, B. Kiefer, M. Strehle and G. Gerber, Controlling the Femtochemistry of $Fe(CO)_5$, *J. Phys. Chem. A*, 1999, **103**, 10381.

29 A. J. Ouderkirk, P. Wermer, N. L. Schultz and E. Weitz, Observation of coordinatively unsaturated intermediates following the pulsed UV photolysis of iron pentacarbonyl ($Fe(CO)_5$), *J. Am. Chem. Soc.*, 1983, **105**, 3354.

30 T. A. Seder, A. J. Ouderkirk and E. Weitz, The wavelength dependence of excimer laser photolysis of $Fe(CO)_5$ in the gas phase. Transient infrared spectroscopy and kinetics of the $Fe(CO)_x$ (x = 4, 3, 2) photofragments, *J. Chem. Phys.*, 1986, **85**, 1977.

31 R. J. Ryther and E. Weitz, Diode laser probes of the product distribution of coordinatively unsaturated iron carbonyls produced following excimer laser photolysis of iron pentacarbonyl in the gas phase, *J. Phys. Chem.*, 1992, **96**, 2561.

32 P. Portius, J. X. Yang, X.-Z. Sun, D. C. Grills, P. Matousek, A. W. Parker, M. Towrie and M. W. George, Unraveling the Photochemistry of $Fe(CO)_5$ in Solution: Observation of $Fe(CO)_3$ and the Conversion between $^3Fe(CO)_4$ and $^1Fe(CO)_4$(Solvent), *J. Am. Chem. Soc.*, 2004, **126**, 10713.

33 R. J. Ryther and E. Weitz, Reaction kinetics of coordinatively unsaturated iron carbonyls formed on gas-phase excimer laser photolysis of iron pentacarbonyl, *J. Phys. Chem.*, 1991, **95**, 9841.

34 V. Bachler, F.-W. Grevels, K. Kerpen, G. Olbrich and K. Schaffner, A Novel Facet of Carbonyl iron-Diene Photochemistry: The η^4-*s-trans* Isomer of the Classical $Fe(CO)_3(\eta^4$-*s-cis*-1,3-butadiene) Discovered by Time-Resolved IR Spectroscopy and Theoretically Examined by Density Functional Methods, *Organometallics*, 2003, **22**, 1696.

35 E. Weitz, Studies of Coordinatively Unsaturated Metal Carbonyls in the Gas Phase by Transient Infrared Spectroscopy, *J. Phys. Chem.*, 1987, **91**, 3945.

36 M.-C. Heitz and C. Daniel, Photodissociation Dynamics of Organometallics: Quantum Simulation for the Dihydride Complex $H_2Fe(CO)_4$, *J. Am. Chem. Soc.*, 1997, **119**, 8269.

37 P. T. Snee, C. K. Payne, S. D. Mebane, K. T. Kotz and C. B. Harris, Dynamics of Photosubstitution Reactions of $Fe(CO)_5$: An Ultrafast Infrared Study of High Spin Reactivity, *J. Am. Chem. Soc.*, 2001, **123**, 6909.

38 J. J. Levison and S. D. Robinson, Transition-metal complexes containing phosphorus ligands. Part II. Triaryl phosphite

derivatives of ruthenium and osmium, *J. Chem. Soc. A*, 1970, 639.

39 T. Ziegler, Coordination geometries and relative donor-acceptor abilities of CX and X_2 (X = O, S, Se, Te) and CX_2 and H_2CX (X = O, S) complexed to $Ru(CO)_4$. Theoretical study by the Hartree-Fock-Slater transition-state method, *Inorg. Chem.*, 1986, **25**, 2721.

40 M. F. Gregory, M. Poliakoff and J. J. Turner, Infrared spectra of ^{13}CO-enriched $Ru(CO)_5$ in liquid xenon: the energy-factored force field, *J. Mol. Struct.*, 1985, **127**, 247.

41 A. W. Ehlers and G. Frenking, Structures and Bond Energies of the Transition-Metal Carbonyls $M(CO)_5$ (M = Fe, Ru, Os) and $M(CO)_4$ (M = Ni, Pd, Pt), *Organometallics*, 1995, **14**, 423.

42 S. A. Decker and M. Klobukowski, The First Carbonyl Bond Dissociation Energies of $M(CO)_5$ and $M(CO)_4(C_2H_2)$ (M = Fe, Ru, and Os): The Role of the Acetylene Ligand from a Density Functional Perspective, *J. Am. Chem. Soc.*, 1998, **120**, 9342.

43 L. A. Barnes, M. Rosi and C. W. Baushlicher Jr, An *ab initio* study of $Fe(CO)_n$, $n = 1$, 5, and $Cr(CO)_6$, *J. Chem. Phys.*, 1991, **94**, 2031.

44 J. Li, G. Schreckenbach and T. Ziegler, A Reassessment of the First Metal-Carbonyl Dissociation Energy in $M(CO)_4$ (M = Ni, Pd, Pt), $M(CO)_5$ (M = Fe, Ru, Os), and $M(CO)_6$ (M = Cr, Mo, W) by a Quasirelativistic Density Functional Method, *J. Am. Chem. Soc.*, 1995, **117**, 486.

45 P. L. Bogdan and E. Weitz, A transient infrared spectroscopy study of coordinatively unsaturated ruthenium carbonyls, *J. Am. Chem. Soc.*, 1989, **111**, 3163.

46 M. Poliakoff and J. J. Turner, Structure and reactions of matrix-isolated tetracarbonyliron(0), *J. Chem. Soc., Dalton Trans.*, 1974, 2276.

47 P. L. Bogdan and E. Weitz, A transient infrared spectroscopy study of coordinatively unsaturated osmium carbonyl compounds, *J. Am. Chem. Soc.*, 1990, **112**, 639.

48 W. Wang, A. A. Narducci, P. G. House and E. Weitz, Gas-Phase Study of the Formation and Dissociation of $Fe(CO)_4H_2$: Kinetics and Bond Dissociation Energies, *J. Am. Chem. Soc.*, 1996, **118**, 8654.

49 L. Banares, T. Baumert, M. Bergt, B. Kiefer and G. Gerber, The ultrafast photodissociation of $Fe(CO)_5$ in the gas phase, *J. Chem. Phys.*, 1998, **108**, 5799.

50 O. Rubner, T. Baumert, M. Bergt, B. Kiefer, G. Gerber and V. Engel, Theoretical analysis of femtosecond excitation and fragmentation dynamics of $Fe(CO)_5$, *Chem. Phys. Lett.*, 2000, **316**, 585.

51 O. Rubner and V. Engel, Fragmentation dynamics of $Fe(CO)_5$ upon femtosecond excitation: a time-dependent statistical description, *Chem. Phys. Lett.*, 1998, **293**, 485.

52 M. Erdmann, O. Rubner, Z. Shen and V. Engel, Time-resolved photoelectron spectroscopy of $Fe(CO)_5$ multiple fragmentation: theoretical considerations, *Chem. Phys. Lett.*, 2001, **341**, 338.

53 P. T. Snee, C. K. Payne, S. D. Mebane, K. T. Kotz and C. B. Harris, Dynamics of Photosubstitution Reactions of $Fe(CO)_5$: An Ultrafast Infrared Study of High Spin Reactivity, *J. Am. Chem. Soc.*, 2001, **123**, 6909.

54 L. A. Barnes, M. Rosi and C. W. Bauschlicher, An *ab initio* study of $Fe(CO)_n$, $n = 1$, 5, and $Cr(CO)_6$, *J. Chem. Phys.*, 1991, **94**, 2031.

55 B. J. Persson, B. O. Roos and K. Pierloot, A theoretical study of the chemical bonding in $M(CO)_x$ (M = Cr, Fe, and Ni), *J. Chem. Phys.*, 1994, **101**, 6810.

56 B. Delley, M. Wrinn and H. P. Luthi, Binding energies, molecular structures, and vibrational frequencies of transition metal carbonyls using density functional theory with gradient corrections, *J. Chem. Phys.*, 1994, **100**, 5785.

57 W. Wang and E. A. Weitz, Theoretical Study of the Reaction $H_2 + Fe(CO)_4 \rightleftharpoons H_2Fe(CO)_4$, *J. Phys. Chem. A*, 1997, **101**, 2358.

58 O. Rubner, V. Engel, M. R. Hachey and C. Daniel, A CASSCF/MR-CCI study of the excited states of $Fe(CO)_5$, *Chem. Phys. Lett.*, 1999, **302**, 489.

59 O. GonzalezBlanco and V. Branchadell, *J. Chem. Phys.*, 1999, **110**, 778.

60 A. Ricca, Heats of formation for $Fe(CO)_n$ (n = 1-4), *Chem. Phys. Lett.*, 2001, **350**, 313.

61 J. N. Harvey and M. Aschi, Modelling spin-forbidden reactions: recombination of carbon monoxide with iron tetracarbonyl, *Faraday Discuss.*, 2003, **124**, 129.

62 S. A. Trushin, W. Fuss, K. L. Kompa and W. E. Schmid, Femtosecond Dynamics of $Fe(CO)_5$ Photodissociation at 267 nm Studied by Transient Ionization, *J. Phys. Chem. A*, 2000, **104**, 1997.

63 P. T. Snee, C. K. Payne, K. T. Kotz, H. Yang and C. B. Harris, Triplet Organometallic Reactivity under Ambient Conditions: An Ultrafast UV Pump/IR Probe Study, *J. Am. Chem. Soc.*, 2001, **123**, 2255.

64 V. Bachler, F.-W. Grevels, K. Kerpen, G. Olbrich and K. Schaffner, A Novel Facet of Carbonyliron-Diene Photochemistry: The η^4-*s-trans* Isomer of the Classical $Fe(CO)_3(\eta^4$-*s-cis*-1,3-butadiene) Discovered by Time-Resolved IR Spectroscopy and Theoretically Examined by Density Functional Methods, *Organometallics*, 2003, **22**, 1696.

65 M. Besora, J. L. Carreón-Macedo, A. J. Cowan, M. W. George, J. N. Harvey, P. Portius, K. L. Ronayne, X. Z. Sun and M. Towrie, A Combined Theoretical and Experimental Study on the Role of Spin States in the Chemistry of $Fe(CO)_5$ Photoproducts, *J. Am. Chem. Soc.*, 2009, **131**, 3583.

66 J. P. Lomont, S. C. Nguyen and C. B. Harris, Ultrafast Studies of Stannane Activation by Triplet Organometallic Photoproducts, *Organometallics*, 2012, **31**, 3947.

67 M. A. Schroeder and M. S. Wrighton, Pentacarbonyliron(0) photocatalyzed hydrogenation and isomerization of olefins, *J. Am. Chem. Soc.*, 1976, **98**, 551.

68 E. A. McNeill and F. R. Scholer, Molecular structure of the gaseous metal carbonyl hydrides of manganese, iron, and cobalt, *J. Am. Chem. Soc.*, 1977, **99**, 6243.

69 R. L. Sweany, *J. Am. Chem. Soc.*, 1981, **103**, 2410.

70 P. J. Krusic, D. J. Jones and D. C. Roe, Photochemical activation of molecular hydrogen by $Fe(CO)_5$, *Organometallics*, 1986, **5**, 456.

71 D. M. Hayes and E. Weitz, A Study of the Kinetics of Reaction of Fe(CO), and Fe(CO),(L) with H_2 and C_2H_4 for L = H_2 and

C_2H_4 by Transient Infrared Spectroscopy: Reactions Relevant to Olefin Hydrogenation Kinetics, *J. Phys. Chem.*, 1991, **95**, 2723.

72 S. K. Nayak, G. J. Farrell and T. J. Burkey, Photosubstitution of Two Iron Pentacarbonyl CO's in Solution *via* a Single-Photon Process: Dependence on Dispersed Ligands and Role of Triplet Intermediates, *Inorg. Chem.*, 1994, **33**, 2236.

73 S. K. Nayak and T. J. Burkey, Photosubstitution of iron pentacarbonyl, with triethylphosphine in cyclohexane: $Fe(CO)_4PEt_3$ and $Fe(CO)_3(PEt_3)_2$ are single-photon products, *Inorg. Chem.*, 1992, **31**, 1125.

74 A. J. Ouderkirk and E. Weitz, The kinetics of reaction of photolytically generated $Fe(CO)_x$ ($x = 2, 3, 4$) with CO, *J. Chem. Phys.*, 1983, **79**, 1089.

75 E. A. Glascoe, K. R. Sawyer, J. E. Shanoski and C. B. Harris, The Influence of the Metal Spin State in the Iron-Catalyzed Alkene Isomerization Reaction Studied with Ultrafast Infrared Spectroscopy, *J. Phys. Chem. C*, 2007, **111**, 8789.

76 J. N. Harvey and R. Poli, Computational study of the spin-forbidden H_2 oxidative addition to 16-electron Fe(0) complexes, *Dalton Trans.*, 2003, 4100.

77 C. Daniel, M. Benard, A. Dedieu, R. Wiest and A. Veillard, Theoretical Aspects of the Photochemistry of Organometallics. 3. Potential Energy Curves for the Photodissociation of Fe(CO), *J. Phys. Chem.*, 1984, **88**, 4805.

78 J. N. Harvey and R. Poli, Computational study of the spin-forbidden H_2oxidative addition to 16-electron Fe(0) complexes, *J. Chem. Soc., Dalton Trans.*, 2003, 4100.

79 J. N. Harvey, Computational study of the energetics of $^3Fe(CO)_4$, $^1Fe(CO)_4$ and $^1Fe(CO)_4(L)$, L = Xe, CH_4, H_2, and CO, *Phys. Chem. Chem. Phys.*, 2006, **8**, 93.

80 F. Bernardi, M. Olivucci and M. A. Robb, Modelling Photochemical Reactivity of Organic Systems — A New Challenge to Quantum Computational Chemistry, *Isr. J. Chem.*, 1993, 265.

81 M. Klessinger, Conical Intersections and the Mechanism of Singlet Photoreactions, *Angew. Chem., Int. Ed. Engl.*, 1995, **34**, 549.

82 F. Bernardi, M. Olivucci and M. A. Robb, Potential energy surface crossings in organic photochemistry, *Chem. Soc. Rev.*, 1996, 321.

83 F. Bernardi, M. Olivucci and M. A. Robb, The role of conical intersections and excited state reaction paths in photochemical pericyclic reaction, *J. Photochem. Photobiol., A*, 1997, **105**, 365.

84 M. Klessinger, Theoretical models for the selectivity of organic singlet and triplet photoreactions, *Pure Appl. Chem.*, 1997, **69**, 773.

85 M. Klessinger and J. Michl, in *Excited States and Photochemistry of Organic Molecules*, VCH Publishers, New York, 1995.

86 F. Weigend and R. Ahlrichs, Balanced basis sets of split valence, triple zeta valence and quadruple zeta valence quality for H to Rn: Design and assessment of accuracy, *Phys. Chem. Chem. Phys.*, 2005, **7**, 3297.

87 M. J. Bearpark, M. A. Robb and H. B. Schlegel, A direct method for the location of the lowest energy point on a potential surface crossing, *Chem. Phys. Lett.*, 1994, **223**, 269.

88 M. J. Frisch, G. W. Trucks, H. B. Schlegel, G. E. Scuseria, M. A. Robb, J. R. Cheeseman, G. Scalmani, V. Barone, B. Mennucci and G. A. Petersson, *et al.*, Gaussian, Inc., Wallingford CT, 2013.

89 C. Daniel, M. Benard, A. Dedieu, R. Wiest and A. Veillard, Theoretical Aspects of the Photochemistry of Organometallics. 3. Potential Energy Curves for the Photodissociation of Fe(CO), *J. Phys. Chem.*, 1984, **88**, 4805.

90 However, it has been shown by Harvey and Aschi that the energy difference between triplet ground state (**Fe-T1-Int**) and the singlet excited state (**Fe-S1-Int**) was estimated to be 8.0 kcal/mol. See: ref. 61.